Biophysical Reviews (2019) 11:409–418
https://doi.org/10.1007/s12551-019-00539-w

REVIEW

Function-related conformational dynamics of G protein–coupled receptors revealed by NMR

Takumi Ueda[1,2] · Yutaka Kofuku[1] · Junya Okude[1] · Shunsuke Imai[1] · Yutaro Shiraishi[1] · Ichio Shimada[1]

Received: 4 April 2019 / Accepted: 26 April 2019 / Published online: 17 May 2019

Abstract

G protein–coupled receptors (GPCRs) function as receptors for various neurotransmitters, hormones, cytokines, and metabolites. GPCR ligands impart differing degrees of signaling in the G protein and arrestin pathways, in phenomena called biased signaling, and each ligand for a given GPCR has a characteristic level of ability to activate or deactivate its target, which is referred to as its efficacy. The ligand efficacies and biased signaling of GPCRs remarkably affect the therapeutic properties of the ligands. However, these features of GPCRs can only be partially understood from the crystallography data, although numerous GPCR structures have been solved. NMR analyses have revealed that GPCRs have multiple interconverting substates, exchanging on various timescales, and that the exchange rates are related to the ligand efficacies and biased signaling. In addition, NMR analyses of GPCRs in the lipid bilayer environment of rHDLs revealed that the exchange rates are modulated by the lipid bilayer environment, highlighting the importance of the function-related dynamics in the lipid bilayer. In this review, we will describe several solution NMR studies that have clarified the conformational dynamics related to the ligand efficacy and biased signaling of GPCRs.

Keywords Nuclear magnetic resonance · Membrane protein · Adrenergic receptor · Opioid receptor · Nanodiscs

G protein–coupled receptors (GPCRs) are one of the largest membrane protein families in eukaryotes and share a structural topology that is characterized by seven transmembrane helices (TMI to TMVII). GPCRs function as receptors of various chemical messengers, including neurotransmitters, hormones, cytokines (chemokines), and metabolites. Over 30% of modern drugs target GPCRs, and currently more than 300 agents are in clinical trials (Hauser et al. 2017).

Growing numbers of GPCR structures have been solved by X-ray crystallography, and the number of cryo-electron microscopy structures of GPCRs in complexes with their binding partners is rapidly increasing. At present, the structures of more than 60 different GPCRs and over 300 of their complexes with different ligands are available, as documented by GPCRdb—a database dedicated to the GPCR family (Pándy-Szekeres et al. 2018). These structures have strongly promoted our understanding of how GPCRs transmit their signals into the cells. However, crystallography data alone cannot fully explain the important features of GPCR signaling as observed. In addition, the observed conformation may not be the major state in the lipid bilayer environment at the physiological temperature. Recent results have suggested that GPCRs are structurally dynamic and exchange between multiple conformations (Gregorio et al. 2017; Kahsai et al. 2011; Manglik et al. 2015; West et al. 2011).

In relation to this point, NMR methods provide information about the dynamics of proteins over a wide range of frequencies, in aqueous solutions at near-physiological temperatures (Ikeya et al. 2018; Mittermaier and Kay 2009; Osawa et al. 2012). Advances in the NMR techniques describing conformational dynamics have revealed that the global and local conformational fluctuations of

This article is part of a Special Issue dedicated to the "2018 Joint Conference of the Asian Biophysics Association and Australian Society for Biophysics" edited by Kuniaki Nagayama, Raymond Norton, Kyeong Kyu Kim, Hiroyuki Noji, Till Böcking, and Andrew Battle.

✉ Ichio Shimada
shimada@iw-nmr.f.u-tokyo.ac.jp

[1] Graduate School of Pharmaceutical Sciences, The University of Tokyo, Hongo, Bunkyo-ku, Tokyo 113-0033, Japan

[2] Precursory Research for Embryonic Science and Technology, Japan Science and Technology Agency, Kawaguchi, Japan

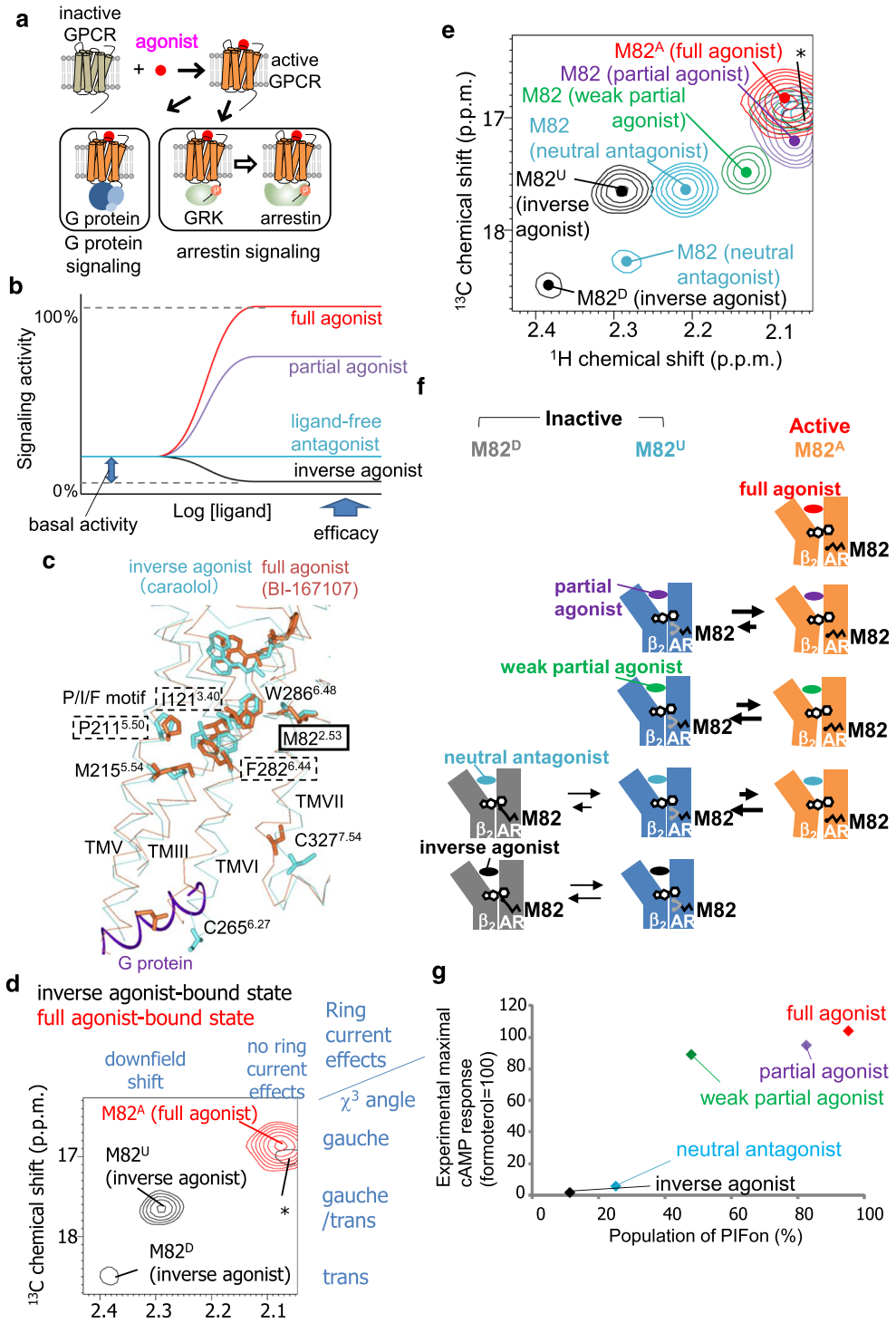

protein structures are closely related to their functions, such as enzymatic activities (Bhabha et al. 2011; Kerns et al. 2015) and molecular recognition (Lange et al. 2008), especially for membrane proteins (Brüschweiler et al. 2015; Minato et al. 2016; Morrison et al. 2011; Nishida et al. 2014).

Although NMR studies of GPCRs are challenging, recent methodological advances have enabled us to observe the NMR signals of various GPCRs, and these NMR studies have revealed that GPCRs exist in function-related equilibria between locally different conformations that are simultaneously populated (Shimada et al. 2018). In this review, we will describe several solution NMR studies that have identified the function-related dynamics of two GPCRs, β_2 adrenergic receptor, and μ-opioid receptor.

◀ **Fig. 1** Ligand efficacy-related conformational dynamics of β_2 adrenergic receptor. **a** Schematic diagram of GPCR signaling. Activated GPCRs induce signal transduction mediated by G proteins. In addition, activated GPCRs may be phosphorylated by GPCR kinases (GRKs), and the phosphorylated GPCRs stimulate G protein-independent signal transduction mediated by arrestin. **b** Plots of signaling activity versus ligand concentration, representing different common GPCR efficacies. **c** The crystal structure of β_2AR with an inverse agonist, carazolol (PDB code: 2RH1) (cyan), and that with a full agonist, BI-167107, and a G protein (PDB code: 3SN6) (orange) are overlaid at TM2 and shown in side views with the extracellular sides on top, viewed from TM6. The middle regions of TM2, TM3, TM5, TM6, and TM7 are shown in Cα traces, and the side-chains of $M82^{2.53}$, $I121^{3.40}$, $P211^{5.50}$, $M215^{5.54}$, $C265^{6.27}$, $F282^{6.44}$, $W286^{6.48}$, and $C327^{7.54}$, and the bound ligands are depicted by sticks. The C-terminal region of the α subunit of the G-protein is shown as a purple ribbon. **d** Overlay of the ^{1}H-^{13}C SOFAST-HMQC spectra of [α,β,β-$^{2}H_3$-, methyl-^{13}C-Met] β_2AR in the carazolol-bound (black) and formoterol-bound (red) states. The relationship between the ^{1}H chemical shifts and the local environments and that between the ^{13}C chemical shifts and the side-chain conformations are shown on the top and right side of the spectra, respectively. **e** Overlay of the ^{1}H-^{13}C SOFAST-HMQC spectra of [α,β,β-$^{2}H_3$-, methyl-^{13}C-Met] β_2AR in the carazolol-bound (black), alprenolol-bound (cyan), tulobuterol-bound (green), clenbuterol-bound (violet), and formoterol-bound (red) states. Only the regions with M82 resonances are shown. The centers of the resonances from M82 are indicated with dots. **f** Proposed mechanism for the various efficacies of β_2AR with different ligands. β_2AR adopts three conformations with different M82 environments: the PIFon conformation, which corresponds to the $M82^{A}$ signal, induces signaling, whereas the $PIFoff_1$ and $PIFoff_2$ conformations, which correspond to the $M82^{U}$ and $M82^{D}$ signals, do not. In the full agonist formoterol–bound state, β_2AR primarily adopts the PIFon conformation, exhibiting almost the full efficacy of β_2AR. In the partial agonist clenbuterol–bound and partial agonist tulobuterol–bound states, β_2AR exists in equilibrium between the PIFon and $PIFoff_2$ conformations, exhibiting significant signaling with reduced efficacies. In the tulobuterol-bound state, where the efficacy is lower than that of the clenbuterol-bound state, the population of the PIFon conformation is smaller. In the neutral antagonist alprenolol–bound state, β_2AR primarily adopts the $PIFoff_1$ and $PIFoff_2$ conformations, in equilibrium with a small population of the PIFon conformation. The presence of the small population of the PIFon conformation accounts for the basal activity of β_2AR. In the inverse agonist carazolol–bound state, β_2AR exists in equilibrium between the $PIFoff_1$ and $PIFoff_2$ conformations, exhibiting the inhibition of the basal activities. **g** Plots of the reported maximum cAMP responses against the population of PIFon in each ligand-bound state, calculated from the M82 signals

Ligand efficacy-related conformational dynamics of β_2 adrenergic receptor

Activated GPCRs induce signal transduction mediated by G proteins, arrestins, and various other effectors (Fig. 1a). GPCRs exhibit basal activities in the absence of the ligands, and each chemical ligand for a GPCR has different levels of ability to activate or inhibit their target, which is commonly referred to as its efficacy. The ligands are classified according to their efficacies, with such descriptions as full agonists, partial agonists, neutral antagonists, and inverse agonists (Fig. 1b), and these differences in the efficacies significantly affect the therapeutic properties of the GPCR ligands. For instance, in the case of drugs that target the β_2-adrenergic receptor (β_2AR), a full agonist offers a clinical advantage over a partial agonist in the treatment of acute severe asthma, although the use of full agonists is associated with more adverse effects (Hanania et al. 2010).

The crystal structures of β_2AR have been solved in the inverse agonist–bound form and the ternary complex form bound to the full agonist and a G protein (Cherezov et al. 2007; Rasmussen et al. 2011). In the ternary complex form, the full agonist induces the repositioning of $P211^{5.50}$, $I121^{3.40}$, and $F282^{6.44}$, which are in the central part of β_2AR, as compared with the inverse agonist–bound form where they are located (Fig. 1c). (Superscripts indicate Ballesteros-Weinstein numbering (Ballesteros and Weinstein 1995). The first and second numbers denote the transmembrane helix number and the residue number relative to the most conserved residue in the helix, which is assigned 50.) These residues are referred to as the P/I/F motif and are widely conserved among the GPCRs. In the ternary complex form, the repositioning of the P/I/F motif accompanies the movement of the intracellular side of TMIII, V, VI, and VII, to form a cavity on the cytoplasmic surface. The C-terminal helix of the engineered G protein was inserted into the cavity. Although these structures indicated the activation mechanism of β_2AR, the mechanism underlying the differences in the efficacy was not clear.

NMR was utilized to examine correlations between the ligand efficacy and the β_2AR conformations (Kofuku et al. 2012). Methionine residues are frequently observed in TMIII, TMV, and TMVI of GPCRs, and these regions exhibit large conformational changes upon activation. In the case of β_2AR, $M82^{2.53}$ exists in the central transmembrane region, and the $M82^{2.53}$ side-chain conformation is sensitive to the activation of the P/I/F motif (Fig. 1c). Therefore, the methionine methyl groups were utilized to investigate the conformation of the TM region of β_2AR, in the presence of compounds with different efficacies for β_2AR. In the inverse agonist–bound state, M82 exhibited two signals, referred to as $M82^{D}$ and $M82^{U}$, respectively (Fig. 1d). In the full agonist–bound state, one M82 signal was observed, with chemical shifts remarkably different from those of $M82^{D}$ and $M82^{U}$. This resonance from M82 in the full agonist–bound state is referred to as $M82^{A}$ (Fig. 1d).

The ^{13}C and ^{1}H chemical shifts of the methionine methyl signals are reportedly affected by the side-chain conformations and the local environments, including the ring current effects from the neighboring aromatic rings (Butterfoss et al. 2010; Perkins and Wüthrich 1979). The side-chain conformation and the local environment that correspond to the chemical shifts of $M82^{U}$ and $M82^{D}$ from NMR studies are in good agreement with the inactive P/I/F motif conformation in the crystal structures of β_2AR in its complexes with inverse agonists, and those of $M82^{A}$ are in good agreement with the active

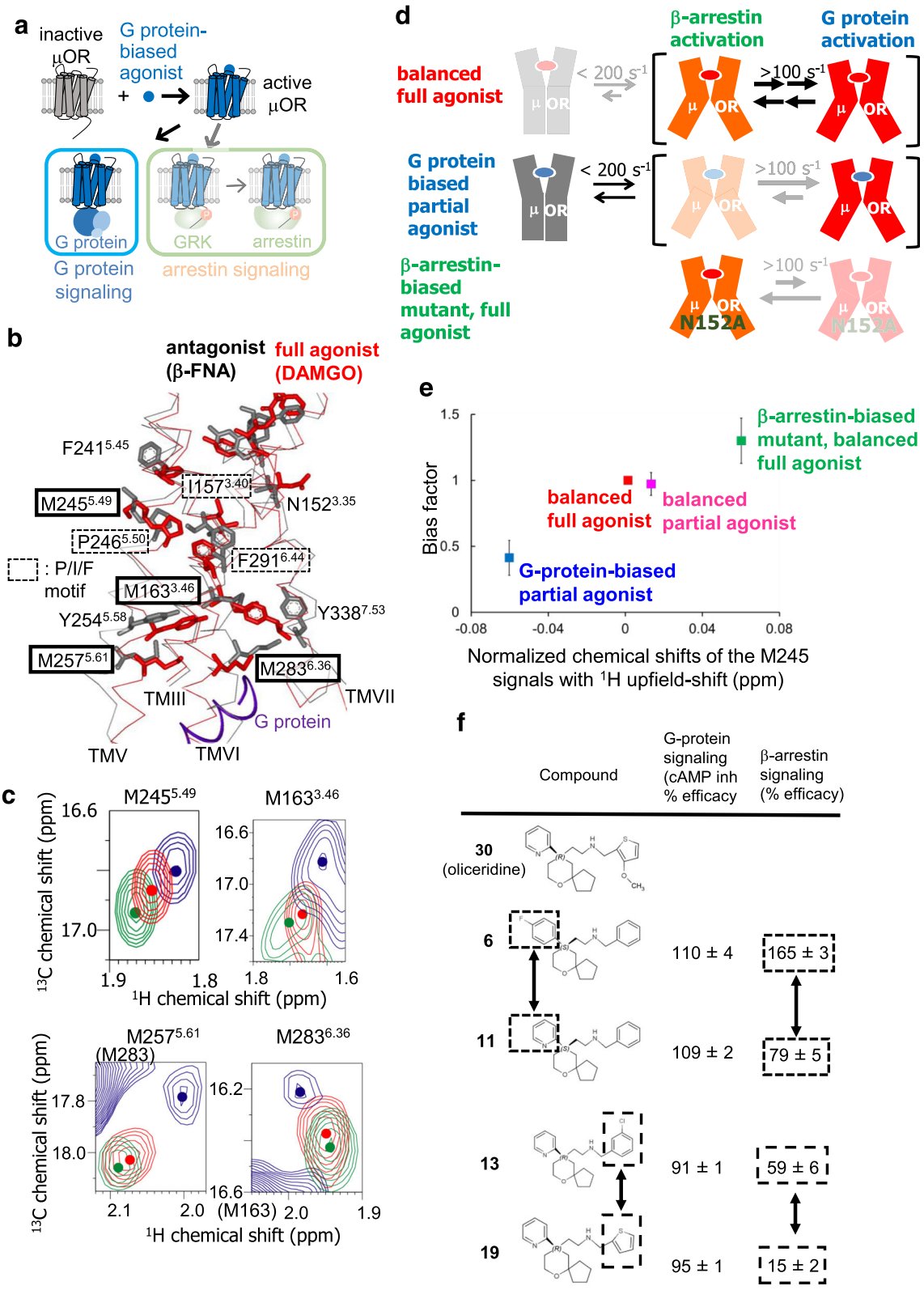

P/I/F motif conformation in the crystal structure of a ternary complex with a full agonist and a G protein. Therefore, the $M82^{U}$ and $M82^{D}$ signals correspond to the inactive P/I/F motif that cannot directly activate G proteins, and the $M82^{A}$ signal corresponds to the active P/I/F motif that can interact with G proteins. These distinct conformations, which correspond to the $M82^{D}$, $M82^{U}$, and $M82^{A}$ signals, are referred to as the $PIFoff_1$, $PIFoff_2$, and PIFon conformations, respectively.

◀ **Fig. 2** Biased signaling–related conformational dynamics of μ-opioid receptor. **a** Schematic diagram of signaling mediated by μOR in the presence of the G protein–biased agonist. **b** The crystal structures of μOR with an irreversible antagonist, β-funaltrexamine (PDB code: 4DKL) (black), and with a full agonist, BU72, and a G protein (PDB code: 6GDG) (red) are shown in side views with the extracellular sides on the upper sides, viewed from TMVI. The middle regions of TMIII, TMV, TMVI, and TMVII are shown in Cα traces, and the side-chains of $N152^{3.35}$, $I157^{3.40}$, $M163^{3.46}$, $F241^{5.45}$, $M245^{5.49}$, $P246^{5.50}$, $M257^{5.61}$, $M283^{6.36}$, $F291^{6.44}$, and $Y338^{7.53}$, and the bound ligands are depicted by sticks. The C-terminal region of the α subunit of the G protein is shown as a red ribbon. **c** Overlaid ^{1}H-^{13}C HMQC spectra of the [^{2}H-8AA, αβ-^{2}H-, methyl-^{13}C-Met] μOR in the DAMGO-bound (red) and oliceridine-bound (blue) states and that of the μOR/$N152^{3.35}$A mutant in the DAMGO-bound state (green). Only the regions with $M245^{5.49}$, $M257^{5.61}$, $M283^{6.36}$, and the ^{1}H upfield-shifted $M163^{3.46}$ resonances are shown. The centers of the resonances from $M163^{3.46}$, $M245^{5.49}$, $M257^{5.61}$, and $M283^{6.36}$ are indicated with dots. **d** Mechanisms leading to the functional selectivity of μOR for different ligands. In the balanced full agonist state with DAMGO bound, μOR primarily adopts the active conformation (red), in which the intracellular surface is characterized by multiple substates with exchange rates larger than 100 s^{-1}. In the G protein–biased partial agonist TRV130–bound state, MOR exists in an equilibrium between the inactive (gray) and active conformations, with exchange rates smaller than 200 s^{-1}, and the equilibrium within the active substates is shifted toward the conformation preferred for G protein activation. In the DAMGO-bound state of the MOR $N152^{3.35}$A mutant, where MOR adopts only the active conformation, the equilibrium among the active substates is shifted toward the conformation preferred for arrestin activation. **e** Correlation between the normalized chemical shifts of the $M245^{5.49}$ NMR signals and the value of the bias factor, which is the ratio of the β-arrestin signaling efficacy to the G protein signaling efficacy. **f** Structure-function relationships of derivatives of the MOR ligand, oliceridine. Modification of either of the two aromatic rings that are highlighted in boxes results in the selective modulation of β-arrestin signaling

In the antagonist-bound state, slightly shifted major and minor resonances from $M82^{U}$ and $M82^{D}$, respectively, were observed (Fig. 1e). For both the weak partial agonist–bound and partial agonist–bound states, a signal was observed at a chemical shift between $M82^{U}$ and $M82^{A}$, such that the chemical shifts from the weak partial agonist–bound state were closer to those of $M82^{U}$ (Fig. 1e). To test if the resonances from $M82^{2.53}$ in the ligand-bound states undergo conformational exchange, lower temperature spectra were recorded at 283 K. As a result, the resonances from $M82^{2.53}$ in the weak partial agonist–bound and partial agonist–bound states significantly shifted away from $M82^{U}$ at 283 K. From this low-temperature measurement resonances, β_2AR exists in an equilibrium between the $PIFoff_1$, $PIFoff_2$, and PIFon conformations.

Based on these structural interpretations of the resonances from $M82^{2.53}$, a signal regulation mechanism was proposed (Fig. 1f). (i) In the full agonist–bound state, most of the β_2AR molecules assume the active conformation. (ii) In the partial agonist–bound states, β_2AR exists in equilibrium between the inactive and active conformations, and the populations of the two conformations determine the efficacies. (iii) In the neutral antagonist alprenolol–bound state, β_2AR exists in equilibrium between two major inactive conformations and one minor active conformation. The weak basal activity is due to the existence of the minor PIFon conformation. (iv) In the inverse agonist–bound state, β_2AR exists in equilibrium between the two locally different inactive conformations. The PIFon populations, calculated from the M82 signals, were correlated with the maximum cAMP levels of cells expressing β_2AR in the presence of the ligands (Fig. 1g), and thus the observed conformational dynamics is related to the ligand efficacy.

Conformational equilibria related to variations in ligand efficacy have been observed in other regions of β_2AR. With CF_3 probes at $C265^{6.27}$ and $C327^{7.54}$ near the cytoplasmic tips of TMVI and TMVII, respectively, equilibria between the inactive and active-like conformations were observed, and the population of the active-like state correlated with the ligand efficacy (Liu et al. 2012). Remarkably, the exchange rates seen for the CF_3 probe at $C265^{6.27}$ were smaller than those observed for the P/I/F motif; i.e., slower than 10 s^{-1}, suggesting that the exchange rates of the P/I/F motif activation are different from those of the conformational exchange near the intracellular surface (Shimada et al. 2018). CPMG experiments with another CF_3 probe, 2-bromo-4-trifluoromethyl-acetanilide, at $C265^{6.27}$ of β_2AR in the apo and inverse agonist–bound states indicated that $C265^{6.27}$ underwent conformational exchange at a rate > 1,000 s^{-1}, suggesting that in the inactive state, the cytoplasmic surface region of β_2AR is characterized as a manifold of rapidly exchanging substates (Manglik et al. 2015; Staus et al. 2016).

Biased signaling-related conformational dynamics of μ-opioid receptor

In addition to the activation of signal transduction mediated by G proteins, GPCRs stimulate G protein-independent signal transduction mediated by arrestin. Various GPCR ligands can modulate signaling through the G protein and arrestin pathways via different mechanisms: GPCR ligands that stimulate both of the signaling pathways and those that preferentially modulate one of the signaling pathways are referred to as "balanced ligands" and "biased ligands," respectively (Urban et al. 2007).

In the case of the μ-opioid receptor (μOR), a GPCR stimulated by various opioid drugs, such as morphine, signaling through the G protein plays a key role in the desired analgesic properties of morphine, whereas signaling through β-arrestin is associated with adverse effects, such as respiratory depression (Bohn et al. 1999). μOR stimulation by oliceridine elicits signaling through Gi, the inhibitory G protein for adenylyl cyclase, but markedly reduces signaling through β-arrestin (Chen et al. 2013) (Fig. 2a). In addition, the N152A mutant of the μ-opioid receptor constitutively activates β-arrestin-

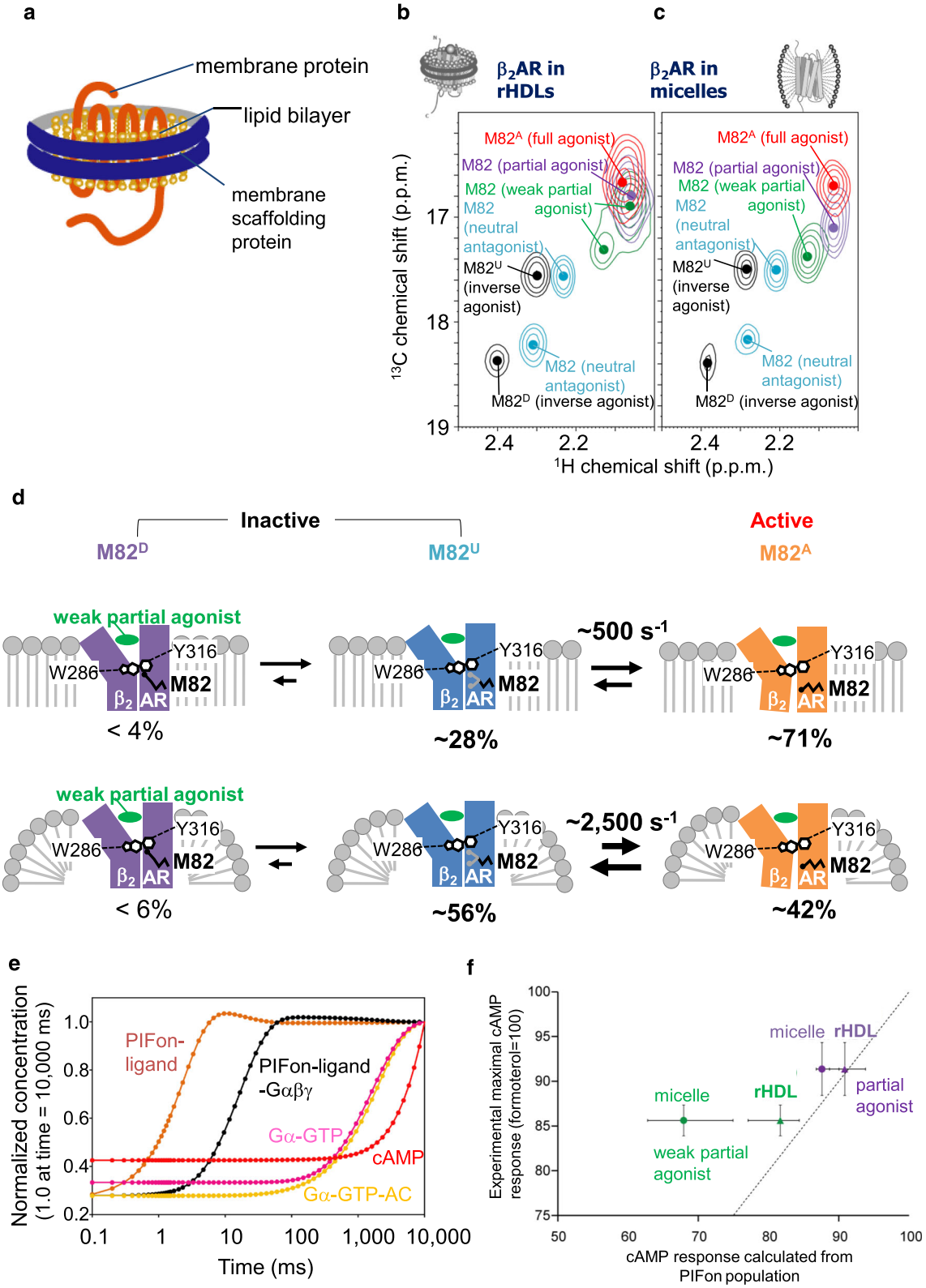

mediated signaling (Fenalti et al. 2014; Okude et al. 2015). G protein–biased ligands of μOR, including oliceridine, reportedly increase the analgesia effects and reduce the on-target adverse effects in comparison with morphine (Chen et al. 2013; Majumdar and Devi 2018). The potential therapeutic applications of the biased signaling of various GPCRs have been proposed (Smith et al. 2018). Therefore, the mechanisms underlying the biased signaling of μOR are important for

◀ **Fig. 3** Function-related dynamics of β_2AR in the lipid bilayer environment. **a** Schematic representation of an rHDL. **b** Overlaid ^{1}H–^{13}C HMQC spectra of [^{2}H-9AA, αβγ-^{2}H-, methyl-^{13}C-Met] β_2AR in rHDLs bound to the inverse agonist carazolol (black), the neutral antagonist alprenolol (cyan), the weak partial agonist tulobuterol (green), the partial agonist clenbuterol (violet), or the full agonist formoterol (red). **c** Overlaid ^{1}H–^{13}C HMQC spectra of [^{2}H-9AA, αβγ-^{2}H-, methyl-^{13}C-Met] β_2AR in DDM micelles, colored as in panel (**b**). In **b** and **c**, only the regions with M82 resonances are shown, and the centers of the M82 resonances are indicated by dots. **d** Differences between the corresponding exchange rates and populations of the conformational substates in β_2AR, in nanodiscs and in DDM micelles. The upper and lower panels depict the conformational equilibria of the β_2AR complex with the weak partial agonist tulobuterol, in nanodiscs and in DDM micelles, respectively. Approximate relative populations of the three states are indicated below the drawings. **e** Simulation of the G protein signaling cascade of β_2AR. Calculated time course of the concentrations of β_2AR in the PIFon conformation, in the G protein-free form (PIFon-ligand), the β_2AR - Gαβγ complex (PIFon-ligand-Gαβγ), the Gα in the GTP-bound form (Gα-GTP), the Gα-adenylate cyclase complex (Gσ-GTP-AC), and cAMP, upon activation by tulobuterol. The concentrations were normalized by those at 10,000 ms. **f** Correlation between the simulated cAMP response based on the PIFon populations observed in the M82 NMR signal and the experimental maximal cAMP responses. Plots of the relative amounts (percentages) of cAMP formed upon activation of CHO-K1 cells by the partial agonists tulobuterol and clenbuterol, which were previously identified as such by cAMP accumulation assays, versus the relative concentration of cAMP in activated cells, calculated from the measured populations of PIFon. Both values were normalized to those in the fully active states and thus are expected to be close to each other whenever the PIFon populations determined by NMR are similar to those in vivo. Circles and triangles represent the cAMP responses, based on the PIFon populations of β_2AR in DDM micelles and in nanodiscs, respectively. The dotted line represents the hypothetical situation where the simulated cAMP response would be equal to the experimental maximal cAMP response. The error bars along the horizontal axis represent the cAMP concentrations, calculated based on the lowest and highest PIFon populations estimated from the M82 NMR signals

understanding the functions of GPCRs and for drug development.

Crystal structures of μOR have been solved in the antagonist-bound form and the ternary complex form composed of μOR, the full agonist, and the G protein-mimicking nanobody (Huang et al. 2015; Manglik et al. 2012). In addition, the cryo-electron microscopy structure of the ternary complex with a full agonist and a G protein has recently been reported (Koehl et al. 2018). Activation-induced conformational changes of the P/I/F motif and the cytoplasmic cavity formation were also observed for the μOR structures. These structures were complemented in important ways by the following NMR studies (Okude et al. 2015).

$M245^{5.49}$ is close to the P/I/F motif and undergoes a conformational change upon activation in human μOR (Fig. 2b). The chemical shifts of $M245^{5.49}$ in the balanced full agonist–bound state were between those of the G protein–biased partial agonist–bound state and those of the β-arrestin-biased mutant bound to the full agonist (Fig. 2c). These results, along with the temperature-dependent shift of these resonances, suggest that μOR adopts multiple active conformations, including the conformations that preferably activate either G protein–mediated signaling or β-arrestin-mediated signaling, that these conformations exchange faster than the chemical shift difference (> 100 s^{-1}), and that the equilibrium is skewed toward the former and latter conformations in the G protein–biased ligand-bound state and the full agonist–bound state of the β-arrestin-biased mutant, respectively (Fig. 2d). The chemical shifts of $M245^{5.49}$ correlate well with the bias factors in each state (Fig. 2e), suggesting that the conformational dynamics of μOR, observed by NMR, are related to the bias factor.

$M163^{3.46}$, $M257^{5.61}$, and $M283^{6.36}$ exist on the intracellular sides of TMIII, TMV, and TMVI (Fig. 2b), and their chemical shifts should be sensitive to the conformational changes of TMVII, as well as TMIII, TMV, and TMVI. The chemical shifts of $M163^{3.46}$, $M257^{5.61}$, and $M283^{6.36}$ also correlate with the bias factor (Fig. 2c), suggesting that the bias factor–dependent conformational equilibrium observed for $M245^{5.49}$ accompanies the coupled conformational changes on the intracellular sides of TMIII, TMV, TMVI, and TMVII.

A comparison of oliceridine derivatives, composed of the 2-[6-oxaspiro[4.5]decan-9-yl] ethylamine scaffold and aromatic groups attached to the oxaspiro[4,5]decan and ethanolamine moieties (Fig. 2f), including compounds 6 to 11 and 13 to 19, revealed that the modification of either of the two aromatic rings results in the selective modulation of β-arrestin signaling (Chen et al. 2013). These structure–activity relationships of the oliceridine derivatives are in agreement with the population shifts of the conformational equilibria that accompany the global conformational changes in TMIII, TMV, TMVI, and TMVII, as revealed by NMR. These relationships between the chemical structures of GPCR ligands and their biased signaling would be helpful for the design of biased ligands.

Function-related dynamics of GPCRs in the lipid bilayer environment

Whereas the β_2AR used in the previous NMR studies was solubilized by detergents, which are widely utilized for structural investigations of membrane proteins, β_2AR is embedded in the lipid bilayer. Reconstituted high-density lipoproteins (rHDLs), also referred to as nanodiscs, can accommodate membrane proteins within a 10-nm-diameter disc-shaped lipid bilayer stabilized by α-helical amphipathic membrane scaffold proteins (MSPs) (Fig. 3a) (Bayburt et al. 2002). The rHDLs reportedly provide a lipid environment with more native-like properties, as compared with liposomes, in terms of the lateral pressure and curvature profiles, since detergent

micelles have strong curvatures and different lateral pressure profiles from lipid membranes.

Although the molecular masses of GPCRs in rHDLs can exceed 200 kDa, the sensitivity enhancement by deuteration enabled the observation of the alanine and methionine methyl groups of β_2AR in rHDLs (Kofuku et al. 2014; Kofuku et al. 2018). In the methyl-TROSY spectra of β_2AR in the weak partial agonist–bound or partial agonist–bound states in rHDLs, $M82^{2.53}$ exhibited resonances with broad and complex lineshapes, suggesting that the exchange rates between the $M82^{D}$, $M82^{U}$, and $M82^{A}$ conformations of β_2AR in rHDLs are lower than those for β_2AR in DDM micelles (Fig. 3b, c). Furthermore, these resonances shifted toward $M82^{A}$, in comparison with those of β_2AR in DDM micelles, suggesting that the population of the $M82^{A}$ conformation of β_2AR in rHDLs is higher than that in DDM micelles (Fig. 3b, c). Based on simulations of the $M82^{2.53}$ resonances in each ligand-bound state of β_2AR, we concluded that the exchange rates between the active and inactive conformations were lower in rHDLs than those in DDM micelles and that the population of the active conformation was higher in rHDLs than that in DDM micelles (Fig. 3d).

A time course simulation of G protein signaling, based on the exchange rates of β_2AR when bound to a neutral antagonist or a weak partial agonist and the previously reported intracellular signaling reaction rates (Saucerman et al. 2003), revealed that the G protein activation and the increase in cAMP occurred on timescales of hundreds of milliseconds and seconds, respectively (Fig. 3e). This is in agreement with the experimentally observed cAMP increases within seconds (Nikolaev et al. 2004) and the G protein–coupled inward rectifier channel activations within hundreds of milliseconds (Bünemann et al. 2001). In the case of receptor tyrosine kinases (RTKs), which also mediate extracellular ligand-dependent cellular responses through multiple intracellular effectors, dimerization and subsequent tyrosine phosphorylation occur on the timescale of seconds to minutes, and thus the signaling from RTKs is slower than that of GPCRs (Swift et al. 2011). The fast conformational change of GPCRs is a result of the preformation of the active conformation, as exemplified by their basal activity, to enable rapid neurotransmission and sensory perception.

The maximum cAMP responses, calculated using the populations of the PIFon conformations of β_2AR in rHDLs, correlated better with the experimental values than those calculated for β_2AR in DDM micelles (Fig. 3f). NMR analyses of other membrane proteins embedded in rHDLs also revealed that the conformational equilibria and the functions of membrane proteins are affected by the lipid bilayer environments (Imai et al. 2012; Minato et al. 2016). Therefore, NMR investigations of GPCRs, as well as other membrane proteins, in the lipid bilayer environments of rHDLs are necessary for accurate measurements of the exchange rates and populations in conformational equilibrium.

Conclusions and future perspectives

As described above, NMR studies have demonstrated that GPCRs exist in function-related conformational equilibria, and the populations of the substates are related to the signaling activities. The information about the function-related conformational equilibria opens an avenue for the rational design of agonists with predictable efficacies and biased signaling. Further NMR analyses for obtaining precise information about the conformation of each substate in the equilibria would provide an answer to the questions of how the GPCR ligands drive the equilibria and how the substates in the equilibria exhibit different signaling activities.

Under physiological conditions, GPCRs are embedded in the lipid bilayers of tissues with various lipid compositions, and the signaling activities of GPCRs can be affected by the lipid compositions of the bilayers. Reconstitution of GPCRs into rHDL lipid bilayers thus will allow for the examination of the effects of various compositions of lipid bilayers on the activities and conformational equilibria of GPCRs by solution NMR experiments.

Acknowledgments This work is supported by The Ministry of Education, Culture, Sports, Science and Technology (MEXT)/Japan Society for the Promotion of Science (JSPS) KAKENHI Grant Numbers JP17H06097, JP18H04540, JP16H01531, JP17H04999, JP16H01353, JP15K18843, JP15J12409, and JP17J1142, and the development of core technologies for innovative drug development based upon IT and the development of innovative drug discovery technologies for middle-sized molecules, from the Japan Agency for Medical Research and Development, AMED (I.S.).

Compliance with ethical standards

Conflict of interest Takumi Ueda declares that he has no conflict of interest. Yutaka Kofuku declares that he has no conflict of interest. Junya Okude declares that he has no conflict of interest. Shunsuke Imai declares that he has no conflict of interest. Yutaro Shiraishi declares that he has no conflict of interest. Ichio Shimada declares that he has no conflict of interest.

Ethical approval This article does not contain any studies with human participants or animals performed by any of the authors.

References

Ballesteros JA, Weinstein H (1995) Integrated methods for the construction of three-dimensional models and computational probing of structure-function relations in G-protein coupled receptors. Methods Neurosci 25:366–428

Bayburt TH, Grinkova YV, Sligar SG (2002) Self-assembly of discoidal phospholipid bilayer nanoparticles with membrane scaffold proteins. Nano Lett 2:853–856

Bhabha G, Lee J, Ekiert DC, Gam J, Wilson IA, Dyson HJ, Benkovic SJ, Wright PE (2011) A dynamic knockout reveals that conformational fuctuations influence the chemical step of enzyme catalysis. Science 332:234–238

Bohn LM, Lefkowitz RJ, Gainetdinov RR, Peppel K, Caron MG, Lin FT (1999) Enhanced morphine analgesia in mice lacking β-arrestin 2. Science 286:2495–2498

Brüschweiler S, Yang Q, Run C, Chou JJ (2015) Substrate-modulated ADP/ATP-transporter dynamics revealed by NMR relaxation dispersion. Nat Struct Mol Biol 22:636–641

Bünemann M, Bücheler MM, Philipp M, Lohse MJ, Hein L (2001) Activation and deactivation kinetics of alpha 2A- and alpha 2C-adrenergic receptor-activated G protein-activated inwardly rectifying K+ channel currents. J Biol Chem 276:47512–47517

Butterfoss GL, DeRose EF, Gabel SA, Perera L, Krahn JM, Mueller GA, Zheng X, London RE (2010) Conformational dependence of ^{13}C shielding and coupling constants for methionine methyl groups. J Biomol NMR 48:31–47

Chen XT, Pitis P, Liu G, Yuan C, Gotchev D, Cowan CL, Rominger DH, Koblish M, Dewire SM, Crombie AL, Violin JD, Yamashita DS (2013) Structure-activity relationships and discovery of a G protein biased μ opioid receptor ligand, [(3-methoxythiophen-2-yl)methyl]({2-[(9R)-9-(pyridin-2-yl)-6-oxaspiro-[4.5]decan- 9-yl]ethyl})amine (TRV130), for the treatment of acute severe pain. J Med Chem 56:8019–8031

Cherezov V, Rosenbaum DM, Hanson MA, Rasmussen SG, Thian FS, Kobilka TS, Choi HJ, Kuhn P, Weis WI, Kobilka BK, Stevens RC (2007) High-resolution crystal structure of an engineered human β_2-adrenergic G protein-coupled receptor. Science 318:1258–1265

Fenalti G, Giguere PM, Katritch V, Huang XP, Thompson AA, Cherezov V, Roth BL, Stevens RC (2014) Molecular control of δ-opioid receptor signalling. Nature 506:191–196

Gregorio GG, Masureel M, Hilger D, Terry DS, Juette M, Zhao H, Zhou Z, Perez-Aguilar JM, Hauge M, Mathiasen S, Javitch JA, Weinstein H, Kobilka BK, Blanchard SC (2017) Single-molecule analysis of ligand efficacy in β_2AR-G-protein activation. Nature 547:68–73

Hanania NA, Dickey BF, Bond RA (2010) Clinical implications of the intrinsic efficacy of β-adrenoceptor drugs in asthma: full, partial and inverse agonism. Curr Opin Pulm Med 16:1–5

Hauser AS, Attwood MM, Rask-Andersen M, Schiöth HB, Gloriam DE (2017) Trends in GPCR drug discovery: new agents, targets and indications. Nat Rev Drug Discov 16:829–842

Huang W, Manglik A, Venkatakrishnan AJ, Laeremans T, Feinberg EN, Sanborn AL, Kato HE, Livingston KE, Thorsen TS, Kling RC, Granier S, Gmeiner P, Husbands SM, Traynor JR, Weis WI, Steyaert J, Dror RO, Kobilka BK (2015) Structural insights into μ-opioid receptor activation. Nature 524:315–321

Ikeya T, Ban D, Lee D, Ito Y, Kato K, Griesinger C (2018) Solution NMR views of dynamical ordering of biomacromolecules. Biochim Biophys Acta 1862:287–306

Imai S, Osawa M, Mita K, Toyonaga S, Machiyama A, Ueda T, Takeuchi K, Oiki S, Shimada I (2012) Functional equilibrium of the KcsA structure revealed by NMR. J Biol Chem 287:39634–39641

Kahsai AW, Xiao K, Rajagopal S, Ahn S, Shukla AK, Sun J, Oas TG, Lefkowitz RJ (2011) Multiple ligand-specific conformations of the β_2-adrenergic receptor. Nat Chem Biol 7:692–700

Kerns SJ, Agafonov RV, Cho YJ, Pontiggia F, Otten R, Pachov DV, Kutter S, Phung LA, Murphy PN, Thai V, Alber T, Hagan MF, Kern D (2015) The energy landscape of adenylate kinase during catalysis. Nat Struct Mol Biol 22:124–131

Koehl A, Hu H, Maeda S, Zhang Y, Qu Q, Paggi JM, Latorraca NR, Hilger D, Dawson R, Matile H, Schertler GFX, Granier S, Weis WI, Dror RO, Manglik A, Skiniotis G, Kobilka BK (2018) Structure of the μ-opioid receptor-G. Nature 558:547–552

Kofuku Y, Ueda T, Okude J, Shiraishi Y, Kondo K, Maeda M, Tsujishita H, Shimada I (2012) Efficacy of the β_2-adrenergic receptor is determined by conformational equilibrium in the transmembrane region. Nat Commun 3:1045

Kofuku Y, Ueda T, Okude J, Shiraishi Y, Kondo K, Mizumura T, Suzuki S, Shimada I (2014) Functional dynamics of deuterated β_2-adrenergic receptor in lipid bilayers revealed by NMR spectroscopy. Angew Chem Int Ed 53:13376–13379

Kofuku Y, Yokomizo T, Imai S, Shiraishi Y, Natsume M, Itoh H, Inoue M, Nakata K, Igarashi S, Yamaguchi H, Mizukoshi T, Suzuki EI, Ueda T, Shimada I (2018) Deuteration and selective labeling of alanine methyl groups of β_2-adrenergic receptor expressed in a baculovirus-insect cell expression system. J Biomol NMR 71(3): 185–192

Lange OF, Lakomek NA, Farès C, Schröder GF, Walter KF, Becker S, Meiler J, Grubmüller H, Griesinger C, de Groot BL (2008) Recognition dynamics up to microseconds revealed from an RDC-derived ubiquitin ensemble in solution. Science 320:1471–1475

Liu JJ, Horst R, Katritch V, Stevens RC, Wüthrich K (2012) Biased signaling pathways in β_2-adrenergic receptor characterized by ^{19}F-NMR. Science 335:1106–1110

Majumdar S, Devi LA (2018) Strategy for making safer opioids bolstered. Nature 553:286–288

Manglik A, Kruse AC, Kobilka TS, Thian FS, Mathiesen JM, Sunahara RK, Pardo L, Weis WI, Kobilka BK, Granier S (2012) Crystal structure of the μ-opioid receptor bound to a morphinan antagonist. Nature 485:321–326

Manglik A, Kim TH, Masureel M, Altenbach C, Yang Z, Hilger D, Lerch MT, Kobilka TS, Thian FS, Hubbell WL, Prosser RS, Kobilka BK (2015) Structural insights into the dynamic process of β_2-adrenergic receptor signaling. Cell 161:1101–1111

Minato Y, Suzuki S, Hara T, Kofuku Y, Kasuya G, Fujiwara Y, Igarashi S, Suzuki E, Nureki O, Hattori M, Ueda T, Shimada I (2016) Conductance of $P2X_4$ purinergic receptor is determined by conformational equilibrium in the transmembrane region. Proc Natl Acad Sci U S A 113:4741–4746

Mittermaier A, Kay L (2009) Observing biological dynamics at atomic resolution using NMR. Trends Biochem Sci 34:601–611

Morrison EA, DeKoster GT, Dutta S, Vafabakhsh R, Clarkson MW, Bahl A, Kern D, Ha T, Henzler-Wildman KA (2011) Antiparallel EmrE exports drugs by exchanging between asymmetric structures. Nature 481:45–50

Nikolaev VO, Bünemann M, Hein L, Hannawacker A, Lohse MJ (2004) Novel single chain cAMP sensors for receptor-induced signal propagation. J Biol Chem 279:37215–37218

Nishida N, Osawa M, Takeuchi K, Imai S, Stampoulis P, Kofuku Y, Ueda T, Shimada I (2014) Functional dynamics of cell surface membrane proteins. J Magn Reson 241:86–96

Okude J, Ueda T, Kofuku Y, Sato M, Nobuyama N, Kondo K, Shiraishi Y, Mizumura T, Onishi K, Natsume M, Maeda M, Tsujishita H, Kuranaga T, Inoue M, Shimada I (2015) Identification of a conformational equilibrium that determines the efficacy and functional selectivity of the μ-opioid receptor. Angew Chem Int Ed Engl 54: 15771–15776

Osawa M, Takeuchi K, Ueda T, Nishida N, Shimada I (2012) Functional dynamics of proteins revealed by solution NMR. Curr Opin Struct Biol 22:660–669

Pándy-Szekeres G, Munk C, Tsonkov TM, Mordalski S, Harpsøe K, Hauser AS, Bojarski AJ, Gloriam DE (2018) GPCRdb in 2018: adding GPCR structure models and ligands. Nucleic Acids Res 46:D440–D446

Perkins SJ, Wüthrich K (1979) Ring current effects in the conformation dependent NMR chemical shifts of aliphatic protons in the basic pancreatic trypsin inhibitor. Biochim Biophys Acta 576:409–423

Rasmussen SG, DeVree BT, Zou Y, Kruse AC, Chung KY, Kobilka TS, Thian FS, Chae PS, Pardon E, Calinski D, Mathiesen JM, Shah ST, Lyons JA, Caffrey M, Gellman SH, Steyaert J, Skiniotis G, Weis WI, Sunahara RK, Kobilka BK (2011) Crystal structure of the β_2 adrenergic receptor-Gs protein complex. Nature 477:549–555

Saucerman JJ, Brunton LL, Michailova AP, McCulloch AD (2003) Modeling beta-adrenergic control of cardiac myocyte contractility in silico. J Biol Chem 278:47997–48003

Shimada I, Ueda T, Kofuku Y, Eddy MT, Wüthrich K (2018) GPCR drug discovery: integrating solution NMR data with crystal and cryo-EM structures. Nat Rev Drug Discov

Smith JS, Lefkowitz RJ, Rajagopal S (2018) Biased signalling: from simple switches to allosteric microprocessors. Nat Rev Drug Discov

Staus DP, Strachan RT, Manglik A, Pani B, Kahsai AW, Kim TH, Wingler LM, Ahn S, Chatterjee A, Masoudi A, Kruse AC, Pardon E, Steyaert J, Weis WI, Prosser RS, Kobilka BK, Costa T, Lefkowitz RJ (2016) Allosteric nanobodies reveal the dynamic range and diverse mechanisms of G-protein-coupled receptor activation. Nature 535:448–452

Swift JL, Godin AG, Doré K, Freland L, Bouchard N, Nimmo C, Sergeev M, De Koninck Y, Wiseman PW, Beaulieu JM (2011) Quantification of receptor tyrosine kinase transactivation through direct dimerization and surface density measurements in single cells. Proc Natl Acad Sci U S A 108:7016–7021

Urban JD, Clarke WP, von Zastrow M, Nichols DE, Kobilka B, Weinstein H, Javitch JA, Roth BL, Christopoulos A, Sexton PM, Miller KJ, Spedding M, Mailman RB (2007) Functional selectivity and classical concepts of quantitative pharmacology. J Pharmacol Exp Ther 320:1–13

West GM, Chien EY, Katritch V, Gatchalian J, Chalmers MJ, Stevens RC, Griffin PR (2011) Ligand-dependent perturbation of the conformational ensemble for the GPCR β_2 adrenergic receptor revealed by HDX. Structure 19:1424–1432